Quasielastic scattering in the inclusive (^{3}He, t) reaction

Neelima G. Kelkar
Istituto Nazionale di Fisica Nucleare, Laboratori Nazionali di Frascati, P.O. Box 13, I-00044 Frascati (Roma), Italy

B. K. Jain
Nuclear Physics Division, Bhabha Atomic Research Centre, Bombay-400085, India

(Received 17 August 1995)

The triton energy spectra of the charge-exchange ^{12}C(^{3}He,t) reaction at 2 GeV beam energy are analyzed in the quasielastic nucleon knockout region. Considering that this region is mainly populated by the charge exchange of a proton in ^{3}He with a neutron in the target nucleus and the final proton going in the continuum, the cross sections are written in the distorted-wave impulse approximation. The t matrix for the elementary exchange process is constructed in the distorted-wave Born approximation, using one-pion-plus-ρ-exchange potential for the spin-isospin nucleon-nucleon potential. This t matrix reproduces the experimental data on the elementary $pn \rightarrow np$ process. The calculated cross sections for the ^{12}C(^{3}He,t) reaction at 2° to 7° triton emission angle are compared with the corresponding experimental data, and are found in reasonable overall accord.

PACS number(s): 13.75.Cs, 24.10.Ht, 24.10.Jv, 25.55.Hp

I. INTRODUCTION

Because of the easy transferability of sufficient energy to the nucleus and the reduced effect of the Pauli blocking, quasifree scattering forms a major portion of the nuclear cross sections at intermediate energies. In experiments, this observation is reflected by the appearance of a distinct broad bump in the ejectile energy spectrum around $\omega = q^2/2m^*$, where $(\omega, \mathbf{q})$ is the four-momentum transfer to the nucleus and m^* the effective mass of the nucleon. The width of this bump is correlated to the momentum spread of the nucleon in the nucleus. In earlier times, this aspect, through the study of the inclusive (p,p'), (e,e') reactions and the exclusive $(p,2p)$, $(e,e'p)$ reactions [1], was exploited much to gather directly information about the single-particle aspect, in particular the shell model, of the nucleus. In recent years, however, the focus on similar studies has shifted to charge-exchange reactions, like (p,n) and (^{3}He,t) [2,3]. This has happened because of the discovery of strong Gamow-Teller excitations in these reactions and a rather simple (Born term) description of the spin-isospin piece of the N-N interaction in terms of a one-pion-plus-ρ-exchange interaction [4]. It is felt that the study of these reactions in the quasifree region, like the earlier quasifree knockout studies, would provide an opportunity to explore the single-particle spin-isospin response of the nucleus and, going beyond, also the particle-hole correlations in the quasifree region. Theorists predict [5] that particle-hole correlations, apart from modifying the magnitudes, shift the longitudinal response towards lower excitation energy and the transverse response towards higher excitation energy. In addition, these correlations are known to renormalize the propagation of pions in the nuclear medium. Because of this, the study of the spin-isospin nuclear response to various external probes has been a topic of great interest over the past decade. An extensive experimental study of the (^{3}He,t) reaction has been carried out at Saturne [6] and the (p,n) reaction at Los Alamos [2]. Theoretically, too, several efforts have been made to study these reactions. Alberico *et al.* [7] have developed a random phase approximatiom (RPA) theory of the spin-isospin nuclear surface response and studied the contrast between the spin-longitudinal (R_L) and spin-transverse (R_T) parts of the nuclear response. Their predictions are for nuclear matter and use a $(\pi+\rho+g')$ model for the interaction. Ichimura *et al.* [8] have improved upon this method and have calculated R_L and R_T by the continuum RPA with the orthogonality condition. They treat the nucleus as of finite size and present the cross sections for a ^{40}Ca(p,p') reaction at $E_p = 500$ MeV using the distorted-wave impulse approximation (DWIA). Notwithstanding these efforts, Bertsch *et al.* [9], however, while discussing a number of experiments in a recent critical review of this field, conclude differently. They find that the effect of the residual particle-hole correlations seen in the experiments in the quasifree region is much smaller than expected.

Considering the above observation of Bertsch *et al.* [9] as an indication of the weakness of the correlations (whatever may be the reason), in the present paper we study the quasielastic peak region as being populated by the charge-exchange knockout of a neutron in the target nucleus. The motivation for this work is to explore the extent up to which the independent particle framework alone could account for the experimental data. We have done the calculations in the DWIA. As a typical case, we analyze the data on the ^{12}C(^{3}He,t) reaction at 2 GeV beam energy [3]. Specifically, we assume that the quasifree region in this reaction is populated by the ^{12}C(^{3}He,tp) reaction, where the proton in the final state arises due to the charge exchange of a proton in ^{3}He with a neutron in $1s_{1/2}$ or $1p_{3/2}$ shell in ^{12}C. Since the experimental data for the ^{12}C(^{3}He,t) reaction in the quasifree region are of inclusive type, in our calculations we do not include the distortion of the proton in the final state. This is

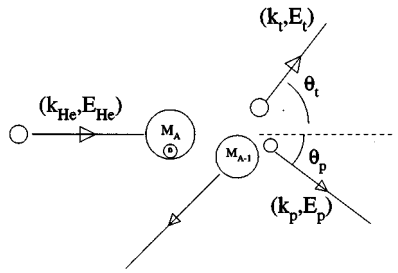

FIG. 1. Diagrammatic representation of the reaction ^{3}He + ^{12}C$\rightarrow t+p+{}^{11}$C.

appropriate, because, as discussed in the literature [12], the main effect of the distortion at intermediate energies is absorptive. This results in the transfer of flux from the given channel to other channels. In an inclusive reaction, these channels are included in the measured cross sections. Also, since the strong absorption of the projectile and ejectile in the nucleus limits the charge exchange between the ^{3}He and ^{12}C nucleons to the low density surface region of the nucleus, we consider the elementary process $pn\rightarrow np$ in the nucleus as a quasifree process. It, of course, is off shell due to nuclear bindings. We construct the t matrix for it following our earlier studies on the elementary processes $p(n,p)n$ and $p(p,\Delta^{++})n$ [10], where the t matrix is constructed in the distorted-wave Born approximation (DWBA), using one-pion-plus-ρ-exchange potential for the $V_{\sigma\tau}$. This t matrix reproduces the experimental data on the $p(n,p)n$ reaction. For the $p(p,\Delta^{++})n$ reaction only one-pion-exchange results agree with the experiments.

In Sec. II we give the formalism for the (^{3}He,t) reaction. The transition amplitude is written in a distorted-wave impulse approximation, as mentioned above, and distortions of ^{3}He and triton are treated in the eikonal approximation. We also present briefly the procedure to calculate the elementary t matrix $t_{\sigma\tau}$.

In the charge-exchange reaction, besides $t_{\sigma\tau}$, the isospin term t_τ also contributes to the cross section. Since in boson-exchange models this t matrix gets constructed from second- and higher-order Born terms only, we have not constructed it here. Alternatively, we have used for it the phenomenologically determined t matrix of Love and Franey [11]. In any case, as we shall see later, the contribution of t_τ to the (^{3}He,t) cross section is not much.

The experimental data for the ^{12}C(^{3}He,t) reaction, as obtained by Bergqvist *et al.* [3], exist for the triton energy spectrum at 2°–7° emission angles and 2 GeV beam energy. These spectra are inclusive. The broad structure seen in them between 1.9 and 2 GeV triton energy can be ascribed to the quasifree charge-exchange reaction. The theoretical cross sections corresponding to these spectra are obtained by first calculating the double-differential cross section $d^2\sigma/d\mathbf{k}_t d\mathbf{k}_p$, and then integrating it over the allowed kinematics of the outgoing protons and summing over the various neutron states in the target nucleus. In Sec. III we present the calculated differential cross sections. The calculations are done with and without the ρ-exchange contribution in the interaction, and compared with the experimentally measured spectra. We find a reasonable overall agreement between the calculated and measured cross sections with pi-plus-rho-exchange interaction.

II. FORMALISM

The differential cross section for the triton energy spectrum in the ^{3}He $+A\rightarrow t+p+B$ reaction in the laboratory is written as

$$\frac{d^2\sigma}{dE_t d\Omega_t}=\int d(\cos\theta_p)\times P\times\langle|T_{BA}|^2\rangle, \tag{1}$$

where $\langle|T_{BA}|^2\rangle$ is the transition amplitude summed and averaged over the spins in the initial and final states, respectively. Factor P includes phase space and the beam flux. Taking the z axis along $\mathbf{k}_{\rm He}$ and the x-z plane defined by the vectors $\mathbf{k}_{\rm He}$ and $\mathbf{k}_t$, it is given by

$$P=\int \frac{d\phi_p}{2(2\pi)^5}\,\frac{k_t k_p^2 m_{\rm He} m_t m_p m_B}{k_{\rm He}[k_p(E_i-E_t)-k_{\rm He}\cos\theta_p E_p+k_t E_p\cos(\theta_{pt})]}, \tag{2}$$

where E_x, k_x, and m_x represent the energy, momentum, and mass, respectively, of the particle x. θ_{pt} is the emission angle of the proton relative to the triton. For a given beam energy and fixed value of the triton four-momentum, k_p is determined by solving the appropriate energy-momentum conservation relations. The cross section $d^2\sigma/dE_t d\Omega_t$ is calculated by integrating over all possible emission directions θ_p and ϕ_p of the outgoing proton.

A. Evaluation of T_{BA}

For the reaction mechanism shown in Fig. 1, the transition amplitude for the reaction A(^{3}He,t)B in the DWIA can be written as

$$T_{BA}=\left\langle \chi^-_{\mathbf{k}_t}\langle t,\{\mathbf{k}_p,B\}|\sum_{ij}\,[t_{\sigma\tau}(i,j)+t_\tau(i,j)]|A,{}^3\mathrm{He}\rangle\chi^+_{\mathbf{k}_{\rm He}}\right\rangle, \tag{3}$$

where j represents the active nucleons in the target nucleus and i those in ^{3}He. The curly brackets in the above equation represent the antisymmetrization between the outgoing proton and the nucleons in the nucleus B. $\chi_{\rm He}$ and χ_t are the distorted waves for helium and triton, respectively. For protons, as mentioned earlier, because of the inclusive nature of the measurements, we use plane waves.

$t_{\sigma\tau}(i,j)$ in Eq. (3) is the spin-isospin t matrix. It contains longitudinal as well as transverse components, and is off shell. In terms of its central $t^{\rm C}$ and noncentral $t^{\rm NC}$ components, we can write it as

$$t_{\sigma\tau}(i,j)=[t^{\rm C}_{\sigma\tau}(\epsilon,\mathbf{q})\sigma_i\cdot\sigma_j+t^{\rm NC}_{\sigma\tau}(\epsilon,\mathbf{q})S_{ij}(\hat{q})]\tau_i\cdot\tau_j, \quad (4)$$

where $\mathbf{q}$ is the momentum transfer in the reaction and ϵ is the energy at which the t matrix needs to be evaluated. Actual evaluation of it is described further below.

The tensor operator $S_{ij}(\hat{q})$ is defined as

$$S_{ij}(\hat{\mathbf{q}})=3\sigma_i\cdot\hat{\mathbf{q}}\sigma_j\cdot\hat{\mathbf{q}}-\sigma_i\cdot\sigma_j=\left(\frac{24\pi}{5}\right)^{1/2}\sum_M\sum_{\mu\nu}(-1)^{\mu+\nu}\sigma_\mu(i)\sigma_\nu(j)\langle 11-\mu-\nu|2M\rangle Y_{2M}(\hat{q}). \quad (5)$$

To evaluate T_{BA}, we first observe that around 2 GeV, the energy of interest of the continuum particles here, the main effect of distortion is absorptive. The dispersive effects are small. Therefore, in evaluating the elementary t matrix $t_{\sigma\tau}$ (or t_τ), we approximate the momentum transfer $\mathbf{q}$ by that corresponding to the asymptotic momenta of ^{3}He and triton. Mathematically, this approximation means writing

$$\begin{aligned}\chi^{-*}_{\mathbf{k}_t}(\mathbf{R}_{aA})\chi^{+}_{\mathbf{k}_{\rm He}}(\mathbf{R}_{aA})&\approx\exp[i\mathbf{q}\cdot\mathbf{R}_{aA}]D_{\mathbf{k}_t}(\mathbf{R}_{aA})D_{\mathbf{k}_{\rm He}}(\mathbf{R}_{aA})=\exp[i\mathbf{q}\cdot(\mathbf{r}_j+\mathbf{x}-\mathbf{r}_i)]D_{\mathbf{k}_t}(\mathbf{r}_j+\mathbf{x}-\mathbf{r}_i)D_{\mathbf{k}_{\rm He}}(\mathbf{r}_j+\mathbf{x}-\mathbf{r}_i)\\&\approx\exp[i\mathbf{q}\cdot(\mathbf{r}_j+\mathbf{x}-\mathbf{r}_i)]D_{\mathbf{k}_t}(\mathbf{r}_j)D_{\mathbf{k}_{\rm He}}(\mathbf{r}_j)=\exp[i\mathbf{q}\cdot(\mathbf{x}-\mathbf{r}_i)]\chi^{-*}_{\mathbf{k}_t}(\mathbf{r}_j)\chi^{+}_{\mathbf{k}_{\rm He}}(\mathbf{r}_j), \quad (6)\end{aligned}$$

where $\mathbf{q}=\mathbf{k}_{\rm He}-\mathbf{k}_t$ and $\mathbf{R}_{aA}$ is the center-of-mass coordinate of t/He relative to the target nucleus. $\mathbf{r}_i$ and $\mathbf{r}_j$ are the coordinates of nucleons in the projectile and target nuclei and $\mathbf{x}$ is the coordinate between these nucleons. D's are the smoothly varying modulating functions describing the distortion of t/He by the nucleus. Dropping their dependence on $\mathbf{r}_i$ and $\mathbf{x}$ in above implies that this dependence does not introduce a significant change in the range of $\mathbf{q}$ at which the ^{3}He$\rightarrow t$ transition density and the elementary $np\rightarrow pn$ t matrix are evaluated.

For ^{3}He and triton wave functions we have used the dominant configuration, which has a symmetric spatial part and a fully antisymmetric spin-isospin part. Since in the calculations we use the ^{3}He$\rightarrow t$ transition density which fit the electron scattering data over a large range of momentum transfer, deficiency, if any, due to P- and D-configuration admixtures in these wave functions should automatically get rectified to a certain extent. With this the $\langle|T_{BA}|^2\rangle$ factorizes as

$$\langle|T_{BA}|^2\rangle=\langle|G|^2\rangle|\rho(\mathbf{q})|^2, \quad (7)$$

where $\rho(\mathbf{q})$ is the spatial ^{3}He$\rightarrow t$ transition density factor and is normalized such that $\rho(0)=3$. For obtaining $\langle|G|^2\rangle$, we take the expectation value of the elementary t matrix over the spin-isospin wave functions of ^{3}He and triton, and then sum and average the square appropriately over the spin projections of these particles. We get

$$\begin{aligned}\langle|G|^2\rangle=\frac{4}{9}\frac{1}{(2J_B+1)}\sum_{m_pM_B}\Bigg\{\sum_{m=-1}^{m=+1}\Bigg[\Bigg|t^{\rm C}_{\sigma\tau}(\epsilon,\mathbf{q})F^{-m,+1}(\mathbf{Q})+\left(\frac{24\pi}{5}\right)^{1/2}t^{\rm NC}_{\sigma\tau}(\epsilon,\mathbf{q})\sum_{\nu M}(-1)^{\nu}\langle 11-m\\-\nu|2M\rangle Y_{2M}(\hat{q})F^{\nu,+1}(\mathbf{Q})\Bigg|^2\Bigg]+|t_\tau(\epsilon,\mathbf{q})|^2|F^{+1}(\mathbf{Q})|^2\Bigg\}. \quad (8)\end{aligned}$$

Here, $\mathbf{Q}=\mathbf{k}_{\rm He}-\mathbf{k}_t-\mathbf{k}_p$ is the momentum of the recoiling nucleus in the laboratory. In the impulse approximation, this momentum equals (with opposite sign) that of the struck neutron in the target nucleus. $F^{\mu,+1}(\mathbf{Q})$ is the ''distorted'' Fourier transform of the spin-isospin overlap integral of the target and residual nucleus. In configuration space, it is given by

$$F^{\mu,+1}(\mathbf{Q})=\int d\mathbf{r}\chi^{-*}_{\mathbf{k}_t}(\mathbf{r})\chi^{+}_{\mathbf{k}_{\rm He}}(\mathbf{r})\langle\mathbf{k}_p|\mathbf{r}\rangle\phi^{BA}_{\mu,+1}(\mathbf{r}), \quad (9)$$

where $\phi^{BA}_{\mu,+1}(\mathbf{r})$ is the overlap integral and is defined through

$$\langle \mathbf{k}_p|\mathbf{r}\rangle \phi^{BA}_{\mu,+1}(\mathbf{r}) = \langle\{\mathbf{k}_p, B\}|\sum_j \delta(\mathbf{r}-\mathbf{r}_j)\sigma_\mu(j)\tau_{+1}|A\rangle. \tag{10}$$

For a shell model and a closed shell target nucleus (i.e., $J_A=0$), it is easy to work out this integral. In this case, for $F^{\mu,+1}(\mathbf{Q})$ we eventually get

$$F^{\mu,+1}(\mathbf{Q}) = \sqrt{6}\sum_{m_s}\sum_{lm_l} \langle l,1/2,m_l,m_s|J_B,-M_B\rangle\langle 1,1/2,\mu,m_s|1/2,m_p\rangle\langle \chi_t^-,\mathbf{k}_p|\chi^+_{\mathrm{He}},\phi_{nljm_l}\rangle. \tag{11}$$

For the purely isospin-dependent term, in a similar way, we obtain

$$\frac{1}{(2J_B+1)}\sum_{M_B m_p}|F^{+1}(\mathbf{Q})|^2 = \sum_{l,m_l}\frac{1}{(2l+1)}|\langle \chi_t^-,\mathbf{k}_p|\chi^+_{\mathrm{He}}\phi_{nljm_l}\rangle|^2. \tag{12}$$

ϕ_{nljm_l} in the above equations is the spatial part of the wave function in the nlj shell of a neutron in the target nucleus. It is normalized such that $\langle\phi_{nljm_l}|\phi_{nljm_l}\rangle = N_{nlj}$, where N_{nlj} is the number of neutrons in the "nlj" shell.

In Eq. (8) one may notice that the contributions of the spin-isospin-dependent and the only isospin-dependent part of the interaction to the cross section enter incoherently. The central and noncentral parts in the spin-isospin interaction, however, add coherently.

B. $p(n,p)n$ t matrix

For constructing the t matrix $t_{\sigma\tau}$, we follow our earlier work [10]. In it, the t matrix for $a\to b$ transition in nucleon-nucleon scattering at intermediate energies is written as

$$t_{ba}(\mathbf{k}_i,\mathbf{k}_f) = (\chi^{-*}_{\mathbf{k}_f},\langle b|V_{\sigma\tau}|a\rangle,\chi^+_{\mathbf{k}_i}), \tag{13}$$

where the effect of elastic and other channels is incorporated through χ's, the distorted waves for the pn relative motion. They are the solutions of potentials which describe the pn elastic scattering. Below the pion threshold, these potentials are available from boson-exchange models. However, in the energy region which is of relevance in the present work and is above the pion threshold, these potentials need major modifications. In the absence of a reliable estimate of such modifications, we have used the eikonal approximation (which is valid at higher energies) and have written χ's directly in terms of the elementary elastic scattering amplitude $f(k,q)$ as (for details see Ref. [13])

$$\chi^+_{\mathbf{k}}(\mathbf{r}) = e^{i\mathbf{k}\cdot\mathbf{r}}\left[1+\frac{i}{k}\int_0^\infty q\,dq J_0(qb)f(k,q)\right]. \tag{14}$$

Here the amplitude $f(k,q)$ peaks at zero degree and falls off rapidly. Near the forward direction it can be reasonably parametrized as [14]

$$f(k,q) = f(k,0)\exp(-\tfrac{1}{2}\alpha q^2), \tag{15}$$

where, using the optical theorem, we can further write

$$f(k,q) = \left(\frac{k}{4\pi}\right)\sigma_T(k)[i+\beta(k)]\exp[-\alpha(k)q^2/2]. \tag{16}$$

Here, σ_T is the total cross section, β is the ratio of the real to imaginary part of the scattering amplitude, and α is the slope parameter in the pn scattering. The values of these parameters depend upon the energy k of the pn system.

The t matrix, with the above parametrization, works out to be

$$t_{ba}(\mathbf{k}_i,\mathbf{k}_f) = \int d\mathbf{r} e^{i\mathbf{q}\cdot\mathbf{r}}\exp[i\xi(b)]\langle b|V_{\sigma\tau}|a\rangle, \tag{17}$$

where $\xi(b)$ is the phase-shift function, and is defined as

$$\exp[i\xi(b)] = [1-C\exp(-b^2/2\alpha)] + iC\beta\exp(-b^2/2\alpha), \tag{18}$$

with $C=\sigma_T/4\pi\alpha$.

$V_{\sigma\tau}$ is the spin-isospin-dependent transition potential. The major portion of this interaction, as is well known [4], arises from the one-pion-plus-rho-exchange potential. We, therefore, write

$$V_{\sigma\tau}(i,j) = [V_\pi(t)\sigma_i\cdot\hat{q}\sigma_j\cdot\hat{q} + V_\rho(t)(\sigma_i\times\hat{q})\cdot(\sigma_j\times\hat{q})]\tau_i\cdot\tau_j, \tag{19}$$

where

$$V_x(t) = -\frac{f_x^2}{3m_x^2}F_x^2(t)\frac{q^2}{m_x^2-t}. \tag{20}$$

$t=\omega^2-q^2$ is the four-momentum transfer. In the $p(n,p)n$ reaction, however, this is same as the three-momentum transfer squared. f_x is the xNN coupling constant, where x denotes π or ρ. $F_x(t)$ is the form factor at the xNN vertex. For its form we use the monopole form, i.e.,

$$F_x(t) = \frac{\Lambda_x^2-m_x^2}{\Lambda_x^2-t}, \tag{21}$$

where Λ is the length parameter.

Substituting Eq. (18) in Eq. (16) the central and noncentral parts of the spin-isospin t matrix, appearing in Eq. (8), work out as

$$t^{\mathrm{C}}_{\sigma\tau}(\mathbf{q}) = \int e^{i\mathbf{q}\cdot\mathbf{r}}e^{i\xi(b)}V^{\mathrm{C}}_{\sigma\tau}(r)d\mathbf{r} \tag{22}$$

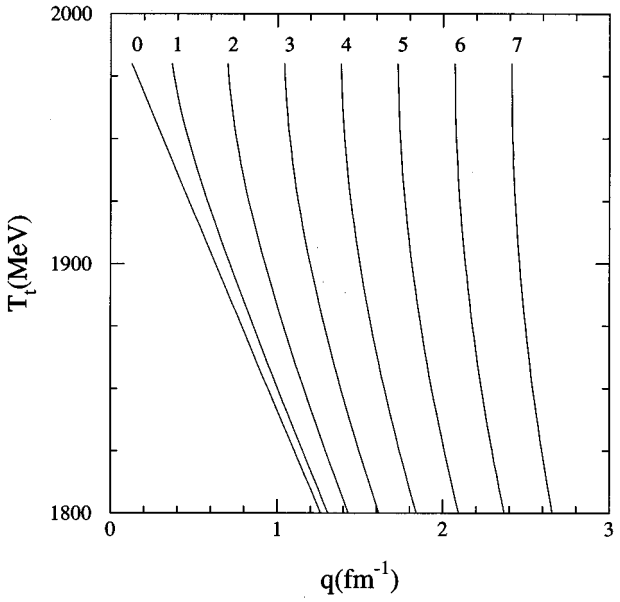

FIG. 2. Kinematics for the ^{12}C(^{3}He,t) reaction at $T_{\rm He}=2$ GeV. The triton energies are plotted as a function of the momentum transfer q, for triton emission angles of 0°–7°.

and

$$t^{\rm NC}_{\sigma\tau}(\mathbf{q})Y_{2M}(\hat{q})=\int e^{i\mathbf{q}\cdot\mathbf{r}}e^{i\xi(b)}V^{\rm NC}_{\sigma\tau}(\mathbf{r})Y_{2M}(\hat{r})d\mathbf{r}, \quad (23)$$

where, in terms of the pi- and rho-exchange potentials, in momentum space

$$V^{\rm C}_{\sigma\tau}(t)=\frac{1}{3}[V_\pi(t)+2V_\rho(t)] \quad (24)$$

and

$$V^{\rm NC}_{\sigma\tau}(t)=\frac{1}{3}[V_\pi(t)-V_\rho(t)]. \quad (25)$$

A detailed presentation of the above t matrix for the elementary charge-exchange reaction and its applicability to the available experimental data over a wide energy range is being reported separately.

III. RESULTS AND DISCUSSION

We calculate the double-differential cross sections for the triton energy spectrum at 2 GeV beam energy and 2°–7° triton emission angles. Within the framework of the formalism given in the preceding sections, various inputs which determine these cross sections are (i) ϕ_{nlj}, the radial wave function of the neutron in the target nucleus, (ii) ^{3}He→t, transition form factor $\rho(q)$, (iii) parameters associated with the pion- and rho-exchange potentials, (iv) parameters of the elastic pn scattering amplitude $f(k,q)$, and (v) ^{3}He and triton distorted waves.

The radial wave functions ϕ_{nlj} are generated in a Woods-Saxon potential, whose parameters are fixed from the analyses of the electron scattering and $(p,2p)$ data on ^{12}C [15]. The neutron binding energies in the $1s_{1/2}$ and $1p_{3/2}$ orbitals in ^{12}C are taken equal to 34 MeV and 16 MeV, respectively.

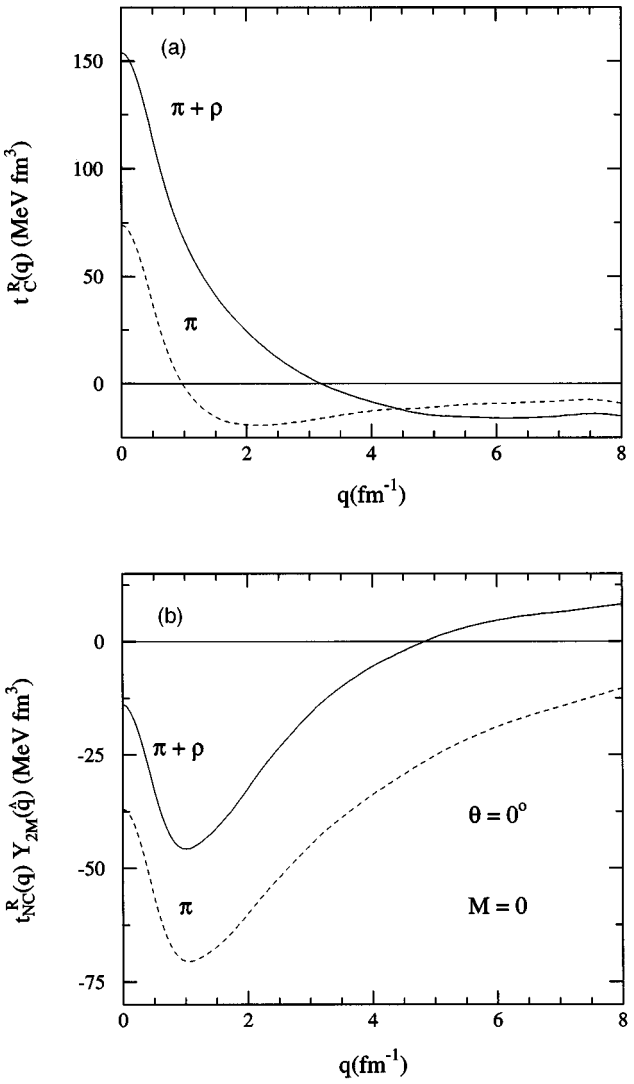

FIG. 3. Real part of the t matrix as a function of the momentum transfer $\mathbf{q}=\mathbf{k}_{\rm He}-\mathbf{k}_t$. Solid curves represent the t matrix constructed with the $\pi+\rho$-exchange transition potential and dashed curves the one-pion exchange only. (a) Central part of the t matrix. (b) Noncentral part of the t matrix.

For the ^{3}He→t transition form factor $\rho(q)$, following the work of Dmitriev *et al.* [16], we use

$$\rho(q)=F_0e^{-\gamma q^2}[1+\eta q^4], \quad (26)$$

where $\gamma=11.15$ GeV^{-2} and $\eta=14$ GeV^{-4}. This form factor has been found to be good up to large momentum transfers.

For the various parameters in the pion- and rho-exchange potentials, we use $f_\pi=1.008$, $f_\rho=7.815$, $\Lambda_\pi=1.2$ GeV/c, and $\Lambda_\rho=2$ GeV/c. These values are consistent with several experimental observations, like πN scattering, NN scattering [17], electrodisintegration of deuterons [18], deuteron properties [19], and dispersive theoretical approaches [20]. The

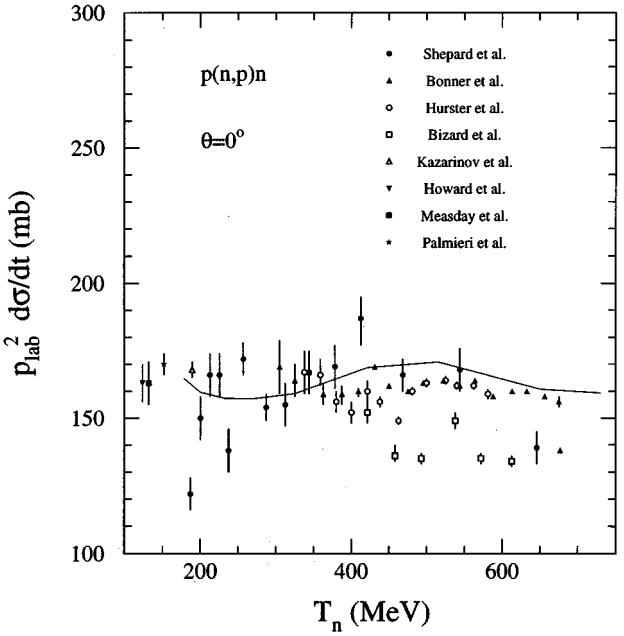

FIG. 4. Calculated and measured $p(n,p)n$ cross sections at 0° for various neutron energies. The calculated cross sections are for the one-pion-plus-rho-exchange spin-isospin potential.

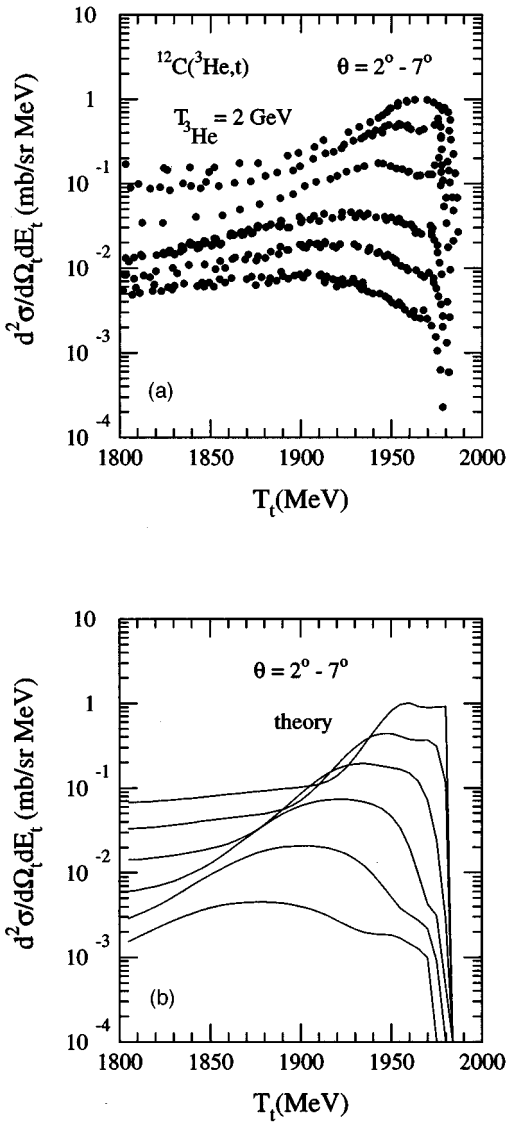

FIG. 5. Triton energy spectra in the quasielastic peak region for ^{12}C(^{3}He,t) at incident beam energy $T_{\rm He}$ = 2 GeV and triton emission angles of 2°–7°. (a) Representation of the experimental data from Ref. [3]. (b) Theoretical calculations with the $\pi+\rho$-exchange transition potential.

value of f_ρ, of course, has some uncertainty. It is 4.83 as determined by the vector dominance model [21], and 7.815 as determined from the nucleon form factor and nuclear phenomena [22].

The elastic pn scattering amplitude $f(k,q)$ has three parameters: the total cross section σ_T, the slope parameter α, which determines its momentum transfer (q) behavior, and the parameter β, which determines the ratio of the real to imaginary parts of $f(k,q)$. Except β, both other parameters are well known from the measured experimental data on the pn scattering [23]. The energy k at which these parameters need to be taken is, of course, not defined well. This happens because of the Fermi motion of the nucleons in the projectile and the target nuclei. However, as the beam energy is high, for the purpose of fixing the values of these parameters, we ignore the Fermi motion of the proton in the beam and the struck neutron in the target. The energy of pn system in the laboratory, therefore, is taken equal to 1/3 of the ^{3}He energy. Corresponding to 2 GeV ^{3}He energy, we find $\alpha\approx 6$ $(\mathrm{GeV}/c)^{-2}$ and $\sigma_T\approx 34$ mb. In the value of β, there exists a lot of uncertainty in the "measured" values [24]. At the energy of our interest, it ranges from 0.05 to -0.7. We have chosen the value -0.45 for our purpose. The calculated cross sections with this value of β are found in most reasonable agreement with the experimental data. We will, of course, exhibit later the sensitivity of our results to the value of β.

For the only isospin-dependent part of the t matrix t_τ, we use the phenomenologically determined t matrix of Love and Franey [11] from NN scattering experiments at 725 MeV beam energy. The contribution of this term to the cross section, however, as we shall see later, is not much.

The distorted waves for helium and triton appear as a product in Eqs. (11), (12). In the eikonal approximation, this can be approximated as

$$\chi_t^{-*}\chi_{\rm He}^{+}=e^{iq_\parallel z}e^{i\mathbf{q}_\perp\cdot\mathbf{b}}e^{2i\delta(b)}, \tag{27}$$

if we ignore the difference between the phase shifts of ^{3}He and triton (around 2 GeV). Here $\delta(b)$ corresponds to the phase shift of a mass 3 particle. The phase shift function $\delta(b)$ can be constructed, in principle, from optical potentials. But since this is a poorly known quantity, we refer to the experimentally measured values. The experimental $\delta(b)$ too is not available for mass 3 particles and hence we use the phase shifts obtained from α scattering at 1.37 GeV on calcium isotopes [25]. Here, $\exp[2i\delta(b)]$, which gives a good description of the α scattering data, is found to be purely real

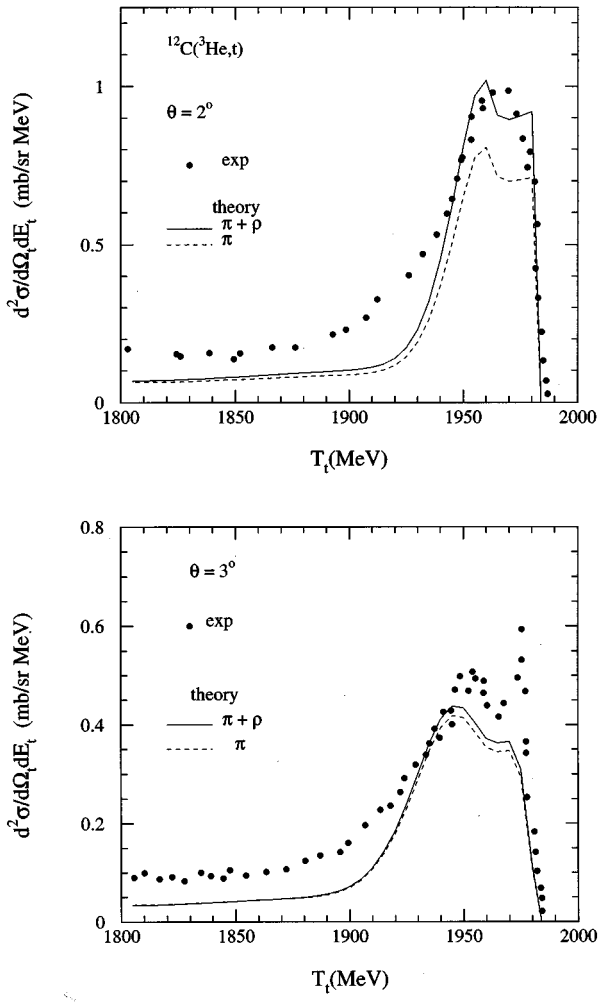

FIG. 6. Triton energy spectra in the quasielastic peak region at triton angles of 2° and 3° for ^{12}C(^{3}He,t) at 2 GeV beam energy. The solid curves are the cross sections with the t matrix consisting of the $\pi+\rho$-exchange transition potential. The dashed curves are the results with only one-pion exchange. Dots represent the experimental data [3].

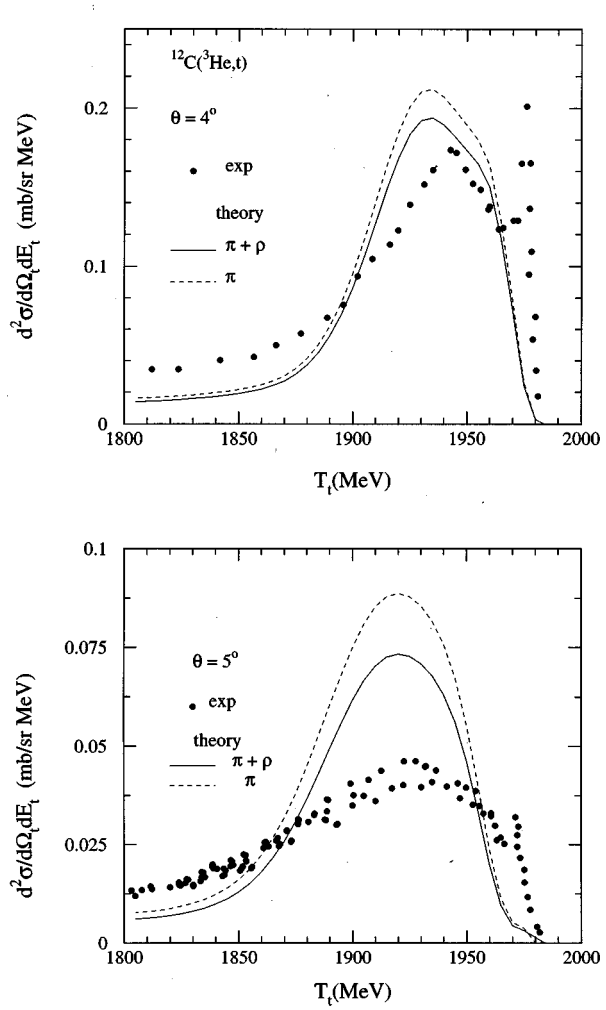

FIG. 7. Same as Fig. 6 for triton emission angles of 4° and 5°.

and has a 1 minus Woods-Saxon form. The radius parameter $r_0(R=r_0A^{1/3})$ and diffuseness a of this functional form are found equal to 1.45 and 0.68 fm, respectively. We use this phase-shift function for our purpose too, except that the radius R is put corresponding to $A=12$.

Before we present the calculated cross sections, in Fig. 2 we show at 2 GeV beam energy the range of momentum transfer (q) involved in the triton emission up to 7° in the laboratory. In the quasielastic range of the triton energy (i.e., up to 1900 MeV), this momentum transfer, as we see, is not small. At 2°–3° it is around 250 MeV/c, and at larger angles it goes to about 500 MeV/c. This suggests that the noncentral component of the t matrix, T_{BA}, and hence the ρ-exchange part of the $V_{\sigma\tau}$ (whose contribution increases at larger q) may affect the quasielastic cross section significantly. However, because the rho exchange contributes with opposite signs to the central and noncentral pieces of the potential [see Eqs. (24), (25)], it is not immediately obvious as how much, in net, the rho exchange would change the cross sections. In Fig. 3 we plot the typical central and noncentral components of the real part of the calculated elementary t matrix [Eqs. (22), (23)] used in our calculations. We show this t matrix for a pure one-pion-exchange potential and for a one-pion-plus-rho-exchange potential. As expected, we see that the rho exchange affects both pieces of the t matrix significantly, but in the opposite directions.

To demonstrate the extent to which the above t matrix reproduces the measured $p(n,p)n$ cross sections, in Fig. 4 we show the calculated 0° cross sections along with the experimental data [26–33] over a large energy range. As we see, the calculated cross sections are in good accord with the measured cross sections.

In Fig. 5 we show the results for the ^{12}C(^{3}He,t) reaction together at all the angles of the triton emission. In Fig. 5(a) we see a representation of the experimentally measured cross sections and in Fig. 5(b) that of our corresponding theoretically calculated results. The calculated cross sections are obtained with the pion and rho meson both included, and with contributions from the spin-flip and non-spin-flip channels to the transition matrix. As can be seen from the figures, the overall behavior of the experimental cross sections, which includes the magnitude and position of the peak and its shift

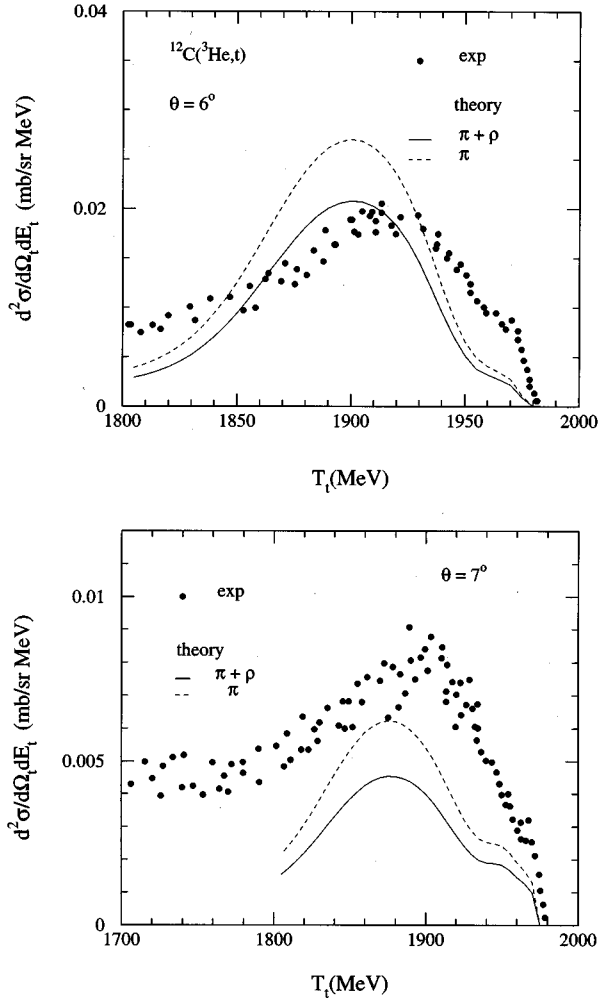

FIG. 8. Same as Fig. 6 for triton emission angles of 6° and 7°.

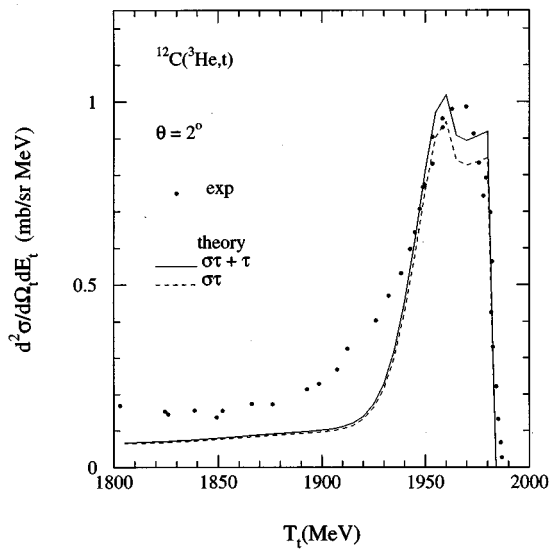

FIG. 9. Comparison of the contribution from the spin-isospin-flip channel (solid curve) and non-spin-flip channel (dashed curve) to the triton energy spectrum at 2° for the ^{12}C(^{3}He,t) reaction at 2 GeV. Dots represent the experimental data [3].

with the emission angle of the triton, gets reproduced reasonably well by the theoretical calculations. This vindicates, in essence, the applicability of the quasifree mechanism framework presented in the earlier section to the region of the triton spectrum lying between the bound nuclear states and the delta production region.

In the following, we give the results at each angle separately.

In Figs. 6, 7, and 8 we show the triton energy spectra plotted individually for six triton emission angles between 2° and 7°. The solid curves represent the calculations with the one-pion-plus-one-rho-exchange interaction. The experimental results are represented by the dots. Except at 5° and 7°, we find a good accord between the calculated and measured cross sections. The underestimation of the cross sections at 7° should not be a source of much discouragement, as the magnitude of the cross section is too small at this angle (~ 7 μb). Therefore, the measured cross section can have a large uncertainty and a significant contribution from other reaction mechanisms. The reason for the overestimation of the cross section by about a factor of 3/2 at 5° is, of course, not clear to us.

To isolate the contribution due to rho exchange to the calculated cross sections, in Figs. 6–8 we also display, by dashed curves, the cross sections due to the one-pion-exchange transition potential alone. As we see from these figures, the contribution of the rho exchange changes continuously from being positive at 2° to negative at 7°. Around 3° it crosses the zero level. This happens, as mentioned earlier, due to change in the momentum transfer q (see Fig. 2) and the opposite signs of the rho-exchange potential in the central and the noncentral pieces of the potential. At smaller momenta, where the central term dominates, the rho exchange comes with a positive sign, while at larger angles, where the noncentral term is important, it comes with a negative sign [see Eqs. (24), (25) and Fig. 3].

In our calculations, we also find that the calculated cross sections are mainly decided by the spin-isospin-dependent part of the t matrix. This can be seen in Fig. 9, where we show the 2° calculated cross sections with and without the isospin-dependent term t_τ. The dashed curve represents the calculation without the isospin-dependent term in the t matrix, while the solid curve is the complete calculation. As we see, the only isospin-dependent term makes a contribution of less than 10% to the cross section.

As we mentioned earlier, the only uncertain parameter in the above calculations had been the value of the parameter β, the ratio of the real to imaginary parts of the elementary scattering amplitude. In Fig. 10 we show the calculated triton energy spectrum at 2° and 6° for three values of β, viz., 0.05, -0.45, and -0.7. These values lie within the uncertainty of the experimentally extracted value. As we see, the calculated cross sections do depend upon the value of β. For the present range, it can change the peak cross section by a factor of 2.

The quasifree cross sections, as we see from the examination of the expression [Eq. (8)] for $\langle |G|^2 \rangle$, is essentially

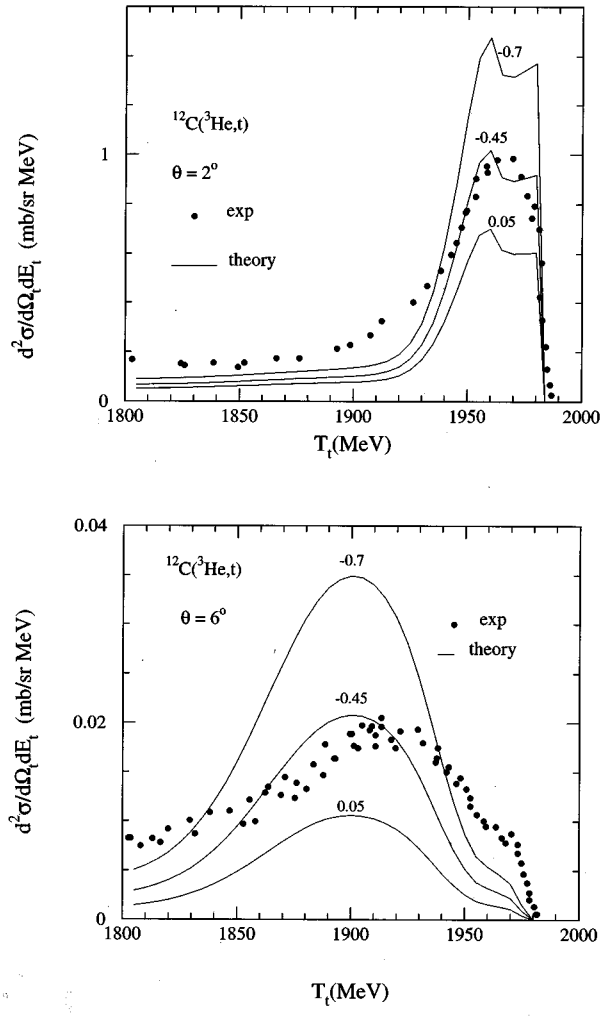

FIG. 10. Triton energy spectra in the quasielastic peak region at triton angles of 2° and 6° for ^{12}C(^{3}He,t) at 2 GeV beam energy for different values of β. The curves are the cross sections with the t matrix consisting of the $\pi+\rho$-exchange transition potential. The numbers on the curves indicate the corresponding values of β.

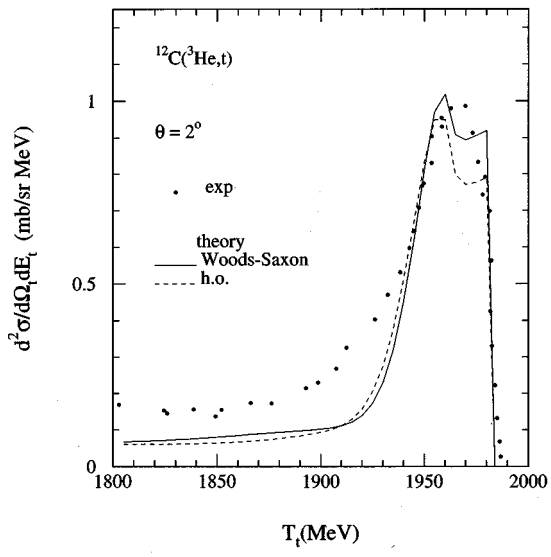

FIG. 11. Triton energy spectrum at triton angle of 2° and 2 GeV beam energy with different forms of the radial wave function ϕ_{nl} of the neutron in the target nucleus.

determined by (i) the t matrix $t_{\sigma\tau}$ and (ii) the neutron momentum distribution in the target nucleus through the recoil momentum distribution factors $F^{\nu,+1}(\mathbf{Q})$ and $F^{+1}(\mathbf{Q})$. The $t_{\sigma\tau}$ depends upon q and F's on $\mathbf{Q}$. In Fig. 2 we see that the magnitude of q, at a particular triton emission angle, does not vary much in the region of the quasielastic peak. At 2° and 3°, for instance, in the triton energy range 1900–1980 MeV the q changes only between 0.7 and 0.9 fm and 1.0 and 1.2 fm, respectively. This means that the elementary t matrix $t_{\sigma\tau}$ too does not change much over this region for a fixed triton emission angle (see Fig. 3). Consequently, in the $A(^3\mathrm{He},t)B$ reaction, the elementary t matrix mainly affects the magnitude of the cross sections (see, e.g., Fig. 10). The shapes of the triton energy spectra, which in the inclusive data mean the peak position and the width, are decided by the recoil momentum distribution factors. However, since in the inclusive data the proton in the final state is not detected and $\mathbf{Q}=\mathbf{k}_{\mathrm{He}}-\mathbf{k}_t-\mathbf{k}_p$, each point in the triton energy spectrum involves an integral over a certain range of $\mathbf{Q}$. This means that even the shape of the triton energy spectra might not depend upon the details of the neutron momentum distribution in the nucleus. It may be sufficient if the neutron wave functions have correct separation energies for different shells and reproduce some gross properties, like the rms radius, of the nucleus. To exhibit this, in Fig. 11 we show the calculated cross sections for two radial wave functions ϕ_{nlj} of the neutron in the target nucleus. The solid curve is the calculation with ϕ_{nlj} generated in a Woods-Saxon potential as has been used throughout this work; the dashed curve is the calculation using the harmonic oscillator wave function with the oscillator parameter $b=1.66$ fm, which is consistent with the electron scattering data. As can be seen from the figure, within about 10%, the two results are the same.

IV. CONCLUSIONS

We have examined the quasielastic peak region in the ^{12}C(^{3}He,t) reaction at 2 GeV over a range of triton emission angles from 2° to 7°. We have calculated the triton energy spectra in the framework of a quasielastic charge exchange between a proton in the projectile and a neutron in the target nucleus. Constructing the t matrix for this process with the $\pi+\rho$-transition potential, and using distorted waves for ^{3}He and triton, the overall features of the experimentally measured cross sections are produced reasonably well. Various inputs used for these calculations are constrained by other known experimental quantities, and thus are not arbitrary.

ACKNOWLEDGMENTS

One of the authors (N.G.K.) wishes to thank the support given by the Department of Atomic Energy, Government of India, for part of the work which was done at the Bhabha Atomic Research Centre in Bombay.

[1] G. Jacob and Th. A. J. Maris, Nucl. Phys. **31**, 139 (1962); Rev. Mod. Phys. **38**, 121 (1966); T. Berggren and H. Tyren, Annu. Rev. Nucl. Sci. **16**, 153 (1966); D. F. Jackson, Adv. Nucl. Phys. **4**, 1 (1971); R. E. Chrien *et al.*, Phys. Rev. C **21**, 1014 (1980); J. S. O'Connell *et al.*, *ibid.* **35**, 1063 (1987).
[2] B. E. Bonner *et al.*, Phys. Rev. C **18**, 1418 (1978); C. Gaarde, Nucl. Phys. **A507**, 79c (1990).
[3] I. Bergqvist *et al.*, Nucl. Phys. **A469**, 648 (1987).
[4] G. E. Brown, J. Speth, and J. Wambach, Phy. Rev. Lett. **46**, 1057 (1981).
[5] W. M. Alberico, M. Ericson, and A. Molinari, Phys. Lett. **92B**, 153 (1980); Nucl. Phys. **A379**, 429 (1982).
[6] D. M. Contardo *et al.*, Phys. Lett. **168B**, 331 (1986); C. Ellegard *et al.*, Phys. Rev. Lett. **50**, 1745 (1983); Phys. Lett. **154B**, 110 (1985); D. Bachelier *et al.*, *ibid.* **172B**, 23 (1986).
[7] W. M. Alberico *et al.*, Phys. Rev. C **38**, 109 (1988).
[8] M. Ichimura *et al.*, Phys. Rev. C **39**, 1446 (1989).
[9] G. F. Bertsch, L. Frankfurt, and M. Strikman, Science **259**, 773 (1993).
[10] B. K. Jain and A. B. Santra, Phys. Rev. C **46**, 1183 (1992); Phys. Rep. **230**, 1 (1993).
[11] W. G. Love and M. A. Franey, Phys. Rev. C **24**, 1073 (1981); M. A. Franey and W. G. Love, *ibid.* **31**, 488 (1985).
[12] N. Austern and C. M. Vincent, Phys. Rev. C **23**, 1847 (1981).
[13] B. K. Jain and A. B. Santra, Nucl. Phys. **A519**, 697 (1990); Phys. Lett. B **244**, 5 (1990).
[14] H. Palevsky *et al.*, Phys. Rev. Lett. **18**, 1200 (1967); G. J. Igo *et al.*, Nucl. Phys. **B3**, 181 (1967); B. A. Ryan *et al.*, Phys. Rev. D **3**, 1 (1971).
[15] L. R. B. Elton and A. Swift, Nucl. Phys. **A94**, 52 (1967); R. Shanta and B. K. Jain, *ibid.* **A175**, 417 (1971).
[16] V. F. Dmitriev, O. Sushkov, and C. Gaarde, Nucl. Phys. **A459**, 503 (1986).
[17] R. Machleidt, K. Holinde, and C. Elster, Phys. Rep. **149**, 1 (1987); W. N. Cottingham *et al.*, Phys. Rev. D **8**, 800 (1973).
[18] J. F. Mathiot, Nucl. Phys. **A412**, 201 (1984).
[19] T. E. O. Ericson and M. Rosa-Clot, Nucl. Phys. **A405**, 497 (1983).
[20] W. Nutt and B. Loiseau, Nucl. Phys. **B104**, 333 (1976).
[21] M. M. Nagels *et al.*, Nucl. Phys. **B109**, 1 (1976).
[22] G. Hohler and E. Pietarinen, Nucl. Phys. **B95**, 210 (1975).
[23] B. H. Silverman *et al.*, Nucl. Phys. **A499**, 763 (1989).
[24] W. Grein, Nucl. Phys. **B131**, 255 (1977).
[25] D. C. Choudhury, Phys. Rev. C **22**, 1848 (1980).
[26] P. F. Shepard, T. J. Devlin, R. E. Mischke, and J. Solomon, Phys. Rev. D **10**, 2735 (1974); R. E. Mischke, P. F. Shepard, and T. J. Devlin, Phys. Rev. Lett. **23**, 542 (1969).
[27] B. E. Bonner *et al.*, Phys. Rev. Lett. **41**, 1200 (1978).
[28] W. Hurster *et al.*, Phys. Lett. **90B**, 367 (1980).
[29] G. Bizard *et al.*, Nucl. Phys. **B85**, 14 (1975).
[30] Yu. M. Kazarinov and Yu. N. Simonov, Zh. Eskp. Teor. Fiz. **43**, 35 (1962) [Sov. Phys. JETP **16**, 24 (1963)].
[31] V. J. Howard *et al.*, Nucl. Phys. **A218**, 140 (1974).
[32] D. F. Measday, Phys. Rev. **142**, 584 (1966).
[33] J. N. Palmieri and J. P. Wolfe, Phys. Rev C **3**, 144 (1971).